CMOS-MEMS Post Processing Compatible Capacitively Transduced GeSi Resonators

Syed Naveed Riaz Kazmi, Tom Aarnink, Cora Salm, and Jurriaan Schmitz
MESA+ Institute for Nanotechnology, Department of Electrical Engineering, University of Twente
Enschede, The Netherlands
Email: c.salm@utwente.nl

***Abstract*— This paper reports on the fabrication, simulation and characterization of post processing compatible poly GeSi MEM resonators. The resonators are fabricated, following a two masks process flow, using 1.5 µm thick low stress, highly conductive in-situ boron doped LPCVD poly $Ge_{0.7}Si_{0.3}$ structural layers. All the process steps are kept below 450 °C to potentially avoid CMOS degradation, a prime concern for post processing compatible MEMS. A narrow gap of ~40 nm is achieved using a sacrificial gap oxide layer between the vibrating structure and the electrodes. The GeSi resonators, square plate and circular disk, are excited in their respective Lamé and Wine glass modes exhibiting the resonance peaks at 47.9 MHz and 72.77 MHz, respectively, with the quality factor around 200,000 in air, the highest reported till date for post processing compatible capacitively transduced resonators.**

***Index Terms*— Poly GeSi, post-processing, quality factor, lamé mode, motional resistance, microelectromechanical resonator.**

I. INTRODUCTION

Microelectromechanical (MEM) resonators are emerging as a potential candidate to replace conventional filtering components such as quartz crystal and surface acoustic wave resonators in the RF and IF stages of wireless communication systems. The MEM components exhibiting high quality factor are advantageous due to their small dimensions and ultra-low power consumption [1]. Researchers have demonstrated an acceptable Q under atmospheric conditions at frequencies surpassing 1 GHz [2,3]. However, a major concern for these resonators is their high series motional resistance (R_m) resulting in high insertion losses. Several ways have been proposed to resolve the issue of motional resistance: The use of dielectric material between the electrode and the resonator [4], mechanically coupling a number of identical resonators in an array [5], increasing applied dc voltage and most importantly the gap reduction [6]. The gap reduction technique is the most promising to overcome this issue as the reduction in R_m goes proportional to the fourth power of transduction gap. [7]

By post processing such MEM resonators on top of foundry fabricated CMOS one can achieve low cost and high performance communication systems. This calls for a change of structural materials, as the monocrystalline and polycrystalline silicon, commonly employed as structural layer in microresonators, require processing incompatible with backend technology [8,9]. Germanium-silicon alloys are an attractive alternative, as they are deposited in polycrystalline form at temperatures below 450 °C [10]; under similar conditions silicon deposits in amorphous form.

In the present work, we report on the fabrication of post-processing compatible MEM resonators below 450 °C with as narrow transduction gap as possible to achieve the goal of low motional resistance.

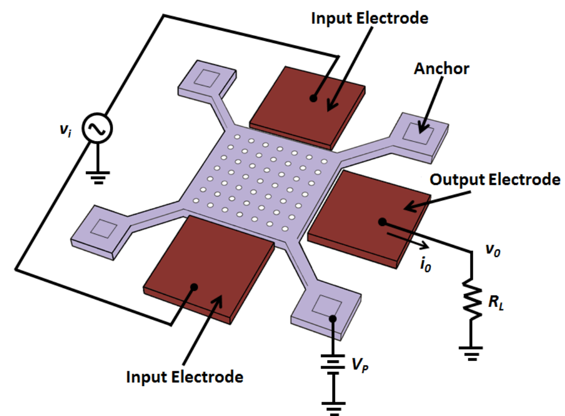

Fig. 1: Perspective schematic view of poly $Ge_{0.7}Si_{0.3}$ capacitively transduced MEM resonator in its two-port excitation and sensing configuration.

II. OPERATION, DESIGN AND SIMULATIONS

Fig. 1 represents the schematic view of a capacitively trasduced resonator in its two-port excitation and sensing configuration. The resonator is excited by applying a dc-bias voltage at the resonator and an ac signal at the input electrodes that are separated by a gap of ~40 nm from the resonator body. The applied ac signal on the input electrodes together with the dc bias at the resonator generates a force in a direction from resonator to electrode, depending on the

This research work is financially supported by Dutch Technology Foundation STW. The authors would like to thank IFCS 2012 for partially meeting the travelling costs for presenting this work.

978-1-4577-1820-5/12/$26.00 ©2012 IEEE

polarity. When the frequency of the input ac signal matches the natural resonance frequency of the resonator, the resonator drives into vibration with a maximum amplitude. The motional current is thus sensed through the output electrode due to the change in capacitance at resonance. The dimensions of the fabricated square plate (SP) and circular disk (CD) resonators are summerizes in Table 1.

TABLE I. DIMENSIONS OF SP AND CD RESONATORS

Parameter	*Symbol*	*Value*
SP Resonator:		
Side length of square plate resonator (µm)	L_{SP}	40
Resonator effective mass (ng)	M_{eff}	9.1
Diameter of release etch holes (µm)	D_{hole}	1.8
Electrode width (µm)	E_w	40
Length of the support beams (µm)	L_s	7.2
Width of the support beams (µm)	W_s	3
CD Resonator:		
Diameter of circular disk resonator (µm)	D_{CD}	20
Resonator effective mass (ng)	M_{eff}	1.3
Electrode width (µm)	E_w	40
Length of the support beams (µm)	L_s	25
Width of the support beams (µm)	W_s	3

The eigenfrequency and frequency response simulations for the SP resonator with the same dimensions as that of fabricated one's is performed in COMSOL finite element modeling software. The Young's modulus value of 91 GPa for highly in-situ boron doped poly $Ge_{0.7}Si_{0.3}$ is obtained from the measured resonance frequency of the released cantilevers, using laser vibrometer. The density of 4110 kg/m^3 is experimentally determined from the weight measurements before and after deposition on the carrier wafer. Fig. 2 represents the simulated Lamé mode of SP resonator, where the adjacent edges vibrate 180° out of phase keeping the volume conserved, using the calculated values of Young's modulus and density for the doped GeSi material. The amplitude of vibration, at resonance, for SP resonator is much exaggerated in this visualization compared to the simulated one, 0.23 Å.

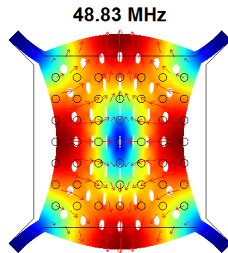

Fig. 2: Eigenfrequency simulation for the Lamé mode of SP poly $Ge_{0.7}Si_{0.3}$ resonator.

III. FABRICATION OF RESONATOR

The MEM resonators presented in this work are fabricated using two mask process on a phosphorus doped carrier wafer of resistivity 1-10 Ω-cm. The main steps for the post-CMOS compatible fabrication process are illustrated in Fig. 3.

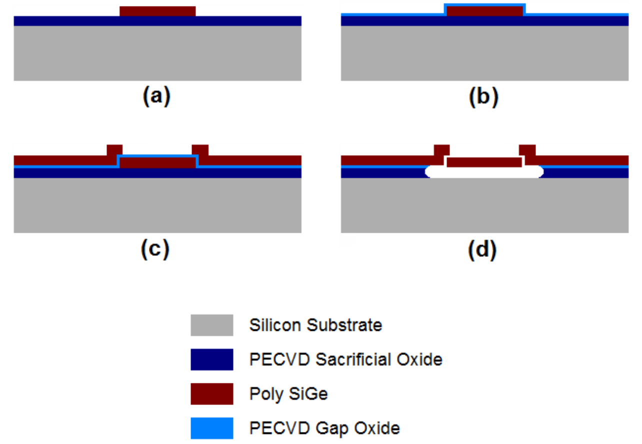

Fig. 3: Two mask process flow for poly GeSi MEM resonators: (a) RIE of 1st poly GeSi structural layer at -90 °C (b) PECVD of oxide to define a gap of ~40 nm (c) patterning of 2nd poly GeSi layer at -75 °C (d) HF vapor etch to release poly GeSi resonator.

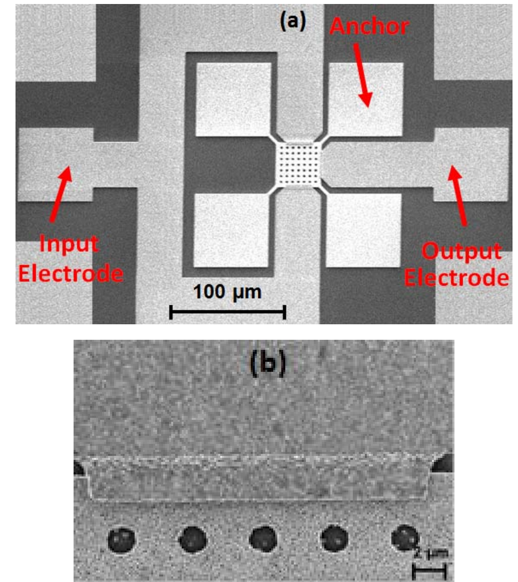

Fig. 4: (a) SEM image of 40x40 µm^2 SP resonator fabricated using the above process flow with 1.8 µm release holes. (b) close-up image of the SP resonator showing the overlap between the resonator body and one of the electrodes.

The fabrication sequence starts with the deposition of an isolation layer of 1.5 µm thick PECVD SiO_2 at 400 °C. Low stress, highly conductive in-situ boron doped poly $Ge_{0.7}Si_{0.3}$ layer (430 °C) [11] of 1.5 µm thickness is then deposited by LPCVD. The resonating structure, support beams and anchor pads are defined by optical lithography and anisotropic reactive ion etching (RIE) in SF_6 and O_2 plasma at -90 °C, Fig. 3a. An SiO_2 layer, Fig. 3b, is then deposited by PECVD (400 °C) to achieve a gap of 40 nm between the resonating body and the electrodes. Next, a second 1.5 µm poly $Ge_{0.7}Si_{0.3}$ layer, using the same recipe as the first structural layer, is deposited on top of gap oxide to serve as the structural layer for the drive and sense electrodes. The RIE of the electrode definition layer includes a considerable over etch given the high topography, and hence requires high selectivity towards SiO_2 - carried out at -75 °C, Fig. 3c. Finally, an HF vapor sacrificial release etch is performed, Fig. 3d.

Fig. 4 shows the SEM images of post-CMOS compatible 47.9 MHz square plate capacitively transduced poly GeSi MEM resonator.

IV. CHARACTERIZATION RESULTS

The electrical characterization of fabricated resonators is performed in a CASCADE probe station. The transmission parameters are measured by a ZVB20 R&S Vector Network Analyzer after performing short-open-load-through (SOLT) calibration on a reference substrate. A direct two-port measurement setup, as shown in Fig. 5, is employed to measure the resonance frequency and Q data for the fabricated resonators. The SP and CD resonators are then excited in their Lamé and Wine glass modes. The grounded substrate allows shunting the feedthrough currents away from the output electrode.

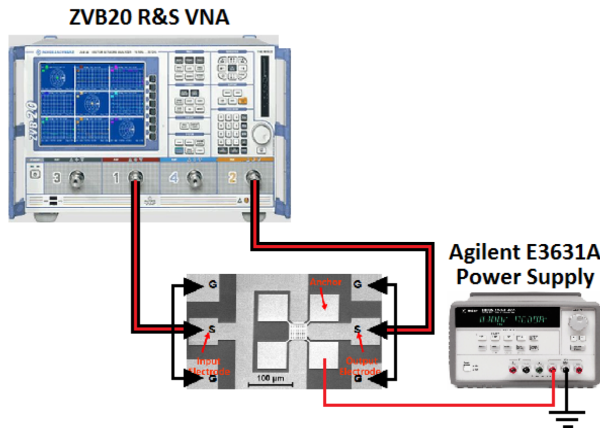

Fig. 5: Measurement setup for the characterization of resonator under atmospheric conditions.

Fig. 6 represents the measured frequency response of a two-port SP resonator under atmospheric conditions. With an input power of -20 dBm at the input electrodes and 3 V dc bias applied at the square plate, a sharp resonance peak is observed at 47.9 MHz.

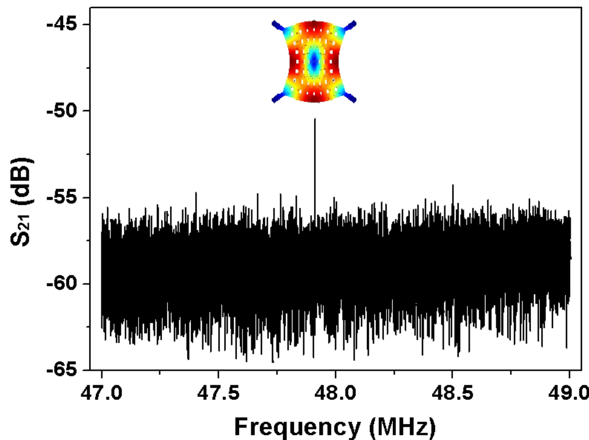

Fig. 6: Measured transmission characteristics of poly $Ge_{0.7}Si_{0.3}$ SP resonator vibrating in its Lamé mode at a bias voltage of 3V. The response is measured over a frequency span of 2 MHz with a frequency step of 100 Hz.

Fig. 7 shows the electrical measurements on the SP resonator with frequency step of 1 Hz. The fabricated resonator exhibits an $f.Q$ product of $1.09 \cdot 10^{13}$, with the quality factor of 228,000 in air, the highest reported till date for post-processing compatible capacitively transduced resonators [4,12]. The resonator exhibits an out-of-band rejection of 6.7 dB and an insertion loss of -50.46 dB. The motional resistance of 33 kΩ is calculated from the S_{21} data for a dc bias of 3V applied over a transduction gap estimated to be 40 nm.

Fig. 8 represents the measured response of a CD resonator with frequency step of 1 Hz. The fabricated resonator exhibits a resonance peak at 72.77 MHz with the quality factor of 185,650 in air. The resonator exhibits an out-of-band rejection of 4.75 dB with an insertion losses of -65.83 dB and the motional resistance of 195 kΩ at a dc bias of 3V. The higher R_m for CD found here is due to the reduced overlap area between the disk and the sense electrode compared to SP resonator.

The high quality factor achieved here, compared to commonly applied alternative thin-film materials, is possibly due to the reduced thermoelastic damping [13] and reduced surface losses [14] caused by the lattice defects and other imperfections that act as sources of energy dissipation in micromechanical resonators.

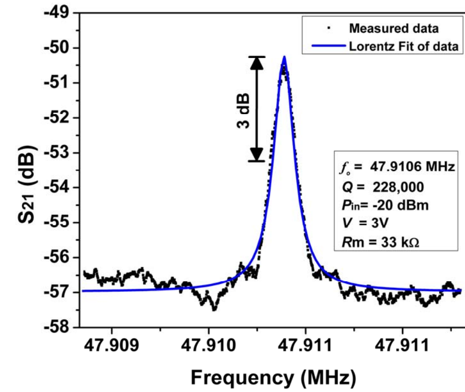

Fig. 7: Measured frequency response of the SP resonator, for a step of 1Hz, exhibiting a resonance peak at f_o= 47.9 MHz with a quality factor of Q= 228,000 in air.

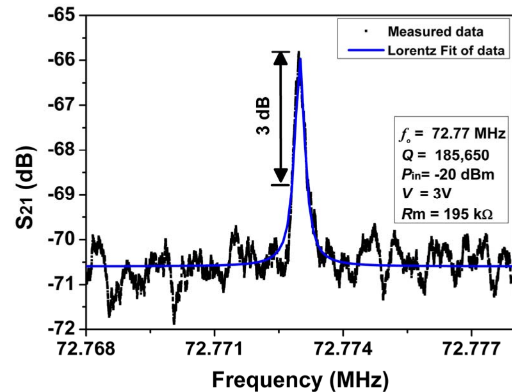

Fig. 8: Frequency response of the CD resonator, for a step of 1Hz, exhibiting a resonance peak at f_o= 72.77 MHz with a quality factor of Q= 185,650 in air.

A reduction of the quality factor for SP resonators is observed with an increased input power level, as shown in Fig. 9. The quality factor drops from 228,000 to 1,050 as input power increases from -20 dBm to -10 dBm. At an even higher input power of 0 dBm the resonance drops in intensity and falls too close to the noise floor to make estimation of the quality factor impossible. A similar degradation trend is observed for CD resonators exhibiting a resonance peak around 72.77 MHz. We expect this degradation might be due to some non-linearities that results in the excitation of spurious modes around the main resonance peak at high input power levels. However, the energy transferred to these spurious modes is still not enough to see them in the measured frequency spectra. The better power handling capability of SP resonator at -10 dBm compared to CD resonator is due to relatively shorter support beams lengths. This attributes to the smaller out-of-plane movement of the SP compared to less constrained CD.

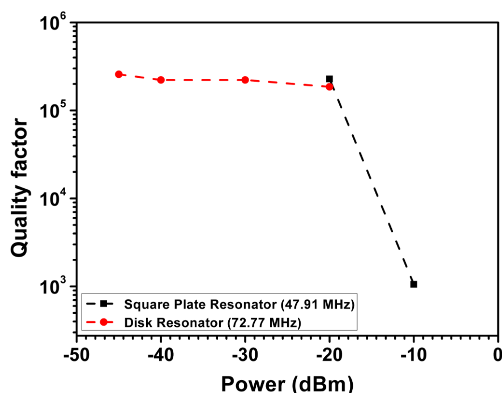

Fig. 9: Input power versus quality factor for SP and CD resonators.

V. CONCLUSIONS

In this work, simulation, fabrication and characterization of two-port capacitively transduced GeSi resonators is carried out. The simulated resonance frequency for these resonators matches within 2% with the measured modes of the fabricated devices. The fabricated resonators exhibit high quality factors around 200,000 under atmospheric conditions. The motional resistance of 33 kΩ is calculated for SP resonators at an input power of -20 dBm and a low dc bias of 3 V. The fabrication of these low power high-Q resonators with a maximum process temperature of 430 °C opens up the feasibility of low cost and high speed RF components on top of foundry fabricated CMOS by post-processing.

ACKNOWLEDGMENTS

The authors would like to thank Milad Darvishi for the useful scientific discussions. We gratefully acknowledge Henk de Vries and Sander Smits for their technical support during RF characterization phase. This work is financially funded by the Dutch Technology Foundation STW through project grant no. 10048 under "CMOS Receiver enhancement using arrays with MEMS" (CREAM).

REFERENCES

[1] C. T.-C. Nguyen, "MEMS technology for timing and frequency control", IEEE Trans. Ultrason., Ferroelectr., Freq. Control, vol. 54, no. 2, pp. 251–270, Feb 2007.

[2] J. Wang, Z. Ren, and C. T.-C. Nguyen, "1.156 GHz self-aligned vibrating micromechanical disk resonator, ", IEEE Trans. Ultrason., Ferroelectr., Freq. Control, vol. 51, no. 12, pp. 1605–1628, 2004.

[3] J. Wang, J. E. Butler, T. Feygelson, and C. T.-C. Nguyen, "1.51 GHz polydiamond micromechanical disk resonator with impedance-mismatched isolating support", Proceedings, 17th Int. IEEE Micro Electro Mechanical Systems Conf., pp. 68–73, 2004.

[4] W.-L. Huang, Z. Ren, and C. T.-C. Nguyen, "Nickle vibrating micromechanical resonator with solid dielectric capacitive-transducer gap", IEEE Int. Freq. Control Symp., pp. 839-847, June 2006.

[5] D. Weinstein, S. A. Bhave, M. Tada, S. Mitarai, and S. Morita, "Mechanical coupling of 2D resonator arrays for MEMS filter applications", IEEE Int. Freq. Control Symp. Joint with European Freq. and Time Forum, pp. 1362-1365, 2007.

[6] E.P. Que´vy, S.A.Bhave, H. Takeuchi, T.-J. King, and R.T.Howe, "Poly-SiGe high frequency resonators based on lithographic definition of nano-gap lateral transducers", Technical Digest IEEE Hilton Head, pp. 360 –363, 2004.

[7] V. Kaajakari, A. T. Alastalo, and T. Mattila, "Electrostatic transducers for micromechanical resonator: free space and solid dielectric", IEEE Trans. Ultrason., Ferroelectr., Freq. Control, vol. 53, Issue. 12, pp. 2484-2489, 2006.

[8] J. Schmitz, "Adding functionality to microchips by wafer post-processing", Nucl. Instr. And Meth. 576(1), pp. 142–149, 2007.

[9] H. Takeuchi, A. Wung, X. Sun, R. T. Howe, and T.-J. King, "Thermal budget limits of quarter-micron foundry CMOS for post-processing MEMS devices," IEEE Trans. on Elec. Devices, vol. 52, no. 9, pp. 2081-2086, 2005.

[10] A. Kovalgin and J. Holleman, "Low-Temperature LPCVD of polycrystalline Ge_xSi_{1-x} films with high germanium content", J. Electrochem. Soc., vol. 153, pp. G363-G371, 2006.

[11] S. N. R. Kazmi, A. A. I. Aarnink, A. Y. Kovalgin, C. Salm, and J. Schmitz, "Low stress in-situ boron doped poly SiGe layers for MEMS modular integration with CMOS", ECS Trans. Vol. 35, Issue. 30, pp. 45–52, 2010.

[12] H. Chandrahalim, S. A. Bhave, E. P. Quévy, and R. T. Howe, "Aqueous transduction of poly-SiGe disk resonators", Proc. Trans. & Eurosensors, pp. 313-316, (2007).

[13] C. Zener, "Internal friction in solids: II. General theory of thermo-elastic internal friction"Phys. Rev. vol. 53, no. 1, pp. 90–99, 1938.

[14] K. Y. Yasumura, T. D. Stowe, E. M. Chow, T. Pfafman, T. W. Kenny, B. Barry, C. Stipe, and D. Rugar, "Quality factors in micron- and submicron-thick cantilevers", J. Microelectromech. Syst., vol. 9, no. 1, pp. 117–125, 2000.